14. Okabayashi T, Hanazaki K. Overwhelming postsplenectomy infection syndrome in adults—a clinically preventable disease. World J Gastroenterol. 2008;14:176–9.
15. Stasi R, Evangelista ML, Amadori S. Novel thrombopoietic agents a review of their use in idiopathic thrombocytopenic purpura. Drugs. 2008;68:901–12.
16. Matthys G, Park JW, McGuire S, Wire MB, Bowen C, Williams D, et al. Clinical pharmacokinetics, platelet response, and safety of eltrombopag at supratherapeutic doses of up to 200 mg once daily in healthy volunteers. J Clin Pharmacol. 2011;51(3):301–8 (Epub 2010 Apr 23).
17. Bussel JB, Cheng G, Saleh MN, Psaila B, Kovaleva L, Meddeb B, et al. Eltrombopag for the treatment of chronic idiopathic thrombocytopenic purpura. N Engl J Med. 2007;357:2237–47.
18. McHutchison JG, Dusheiko G, Shiffman ML, Rodriguez-Torres M, Sigal S, Bourliere M, et al. Eltrombopag for thrombocytopenia in patients with cirrhosis associated with hepatitis C. N Engl J Med. 2007;357:2227–36.
19. Cheng G, Saleh MN, Marcher C, Vasey S, Mayer B, Aivado M, et al. Eltrombopag for management of chronic immune thrombocytopenia (RAISE): a 6-month, randomized, phase 3 study. Lancet. 2011;377:393–402.
20. Bauman JW, Vincent CT, Peng B, Wire MB, Williams DD, Park JW. Effect of hepatic or renal impairment on eltrombopag pharmacokinetics. J Clin Pharmacol. 2011;51:739–50.
21. Gibiansky E, Zhang J, Williams D, Wang Z, Ouellet D. Population pharmacokinetics of eltrombopag in healthy subjects and patients with chronic idiopathic thrombocytopenic purpura. J Clin Pharmacol. 2011;51:842–56.
22. Heddle NM, Cook RJ, Tinmouth A, Kouroukis CT, Hervig T, Klapper E, et al. A randomized controlled trial comparing standard- and low-dose strategies for transfusion of platelets (SToP) to patients with thrombocytopenia. Blood. 2009;113:1564–73.
23. Wai CT, Greenson JK, Fontana RJ, Kalbfleisch JD, Marrero JA, Conjeevaram HS, et al. A simple noninvasive index can predict both significant fibrosis and cirrhosis in patients with chronic hepatitis C. Hepatology. 2003;38(2):518–26.
24. The Japanese Society of Gastroenterology, editor. Liver cirrhosis practical guideline. Tokyo: Nankodo Co. Ltd.; 2009.
25. Drinka PJ, Langer E. The Cockroft–Gault formula. J Am Geriatr Soc. 1989;37(8):820.
26. Farrell C, Hayes S, Giannini EG, Afdhal NH, Tayyab GN, Mohsin A, et al. Gender, race, and severity of liver disease influence eltrombopag exposure in thrombocytopenic patients with chronic liver disease. Hepatology. 2010;52:920A.
27. Shida Y, Takahashi N, Nohda S, Hirama T. Pharmacokinetics and pharmacodynamics of eltrombopag in healthy Japanese males. Jpn J Clin Pharmacol Ther. 2011;42:11–20.
28. Zhang A, Xing Q, Qin S, Du J, Wang L, Yu L, et al. Intra-ethnic differences in genetic variants of the UGT-glucuronosyltransferase1A1 gene in Chinese populations. Pharmacogenomics J. 2007;7:333–8.
29. Mizutani T. PM frequencies of major CYPs in Asians and Caucasians. Drug Metab Rev. 2003;35:99–106.
30. Afdhal N, Giannini E, Tayyab GN, Mohsin A, Lee JW, Andriulli A, et al. Eltrombopag in chronic liver disease patients with thrombocytopenia undergoing an elective procedure: results from ELEVATE, a randomized clinical trial. J Hepatol. 2010;52:S460 (Abstr 1185).
31. Cines DB, Blanchette V. Immune thrombocytopenic purpura. N Engl J Med. 2002;346:995–1008.
32. Giannini EG, Savarino V. Thrombocytopenia in liver disease. Curr Opin Hematol. 2008;15:473–80.
33. Giannini EG, Afdal NH, Campbell FM, Blackman NJ, Shi W, Hyde DK, et al. Exploratory analyses of predictors of thrombotic events in the ELEVATE study. Hepatology. 2010;52:1071A (Abstr 1569).
34. Boilard E, Nigrovic PA, Larabee K, Watts GFM, Ciblyn JS, Weinblatte ME, et al. Platelets amplify inflammation in arthritis via collagen-dependent microparticle production. Science. 2010;327:580–3.
35. Afdhal N, Dusheiko G, Giannini EG, Chen P, Han K, Moshin A, et al. Final results of ENABLE 1, a phase 3, multicenter study of eltrombopag as an adjunct for antiviral treatment of hepatitis C virus-related chronic liver disease associated with thrombocytopenia. Hepatology. 2011;54:1427A–28A (LB-3 Abstract form).

Use of Illumina Deep Sequencing Technology To Differentiate Hepatitis C Virus Variants

Masashi Ninomiya,[a] Yoshiyuki Ueno,[a] Ryo Funayama,[b] Takeshi Nagashima,[b] Yuichiro Nishida,[b] Yasuteru Kondo,[a] Jun Inoue,[a] Eiji Kakazu,[a] Osamu Kimura,[a] Keiko Nakayama,[b] and Tooru Shimosegawa[a]

Division of Gastroenterology, Tohoku University of Medicine, Sendai, Japan,[a] and Division of Cell Proliferation, Tohoku University of Medicine, Sendai, Japan[b]

Hepatitis C virus (HCV) is a positive-strand enveloped RNA virus that shows diverse viral populations even in one individual. Though Sanger sequencing has been used to determine viral sequences, deep sequencing technologies are much faster and can perform large-scale sequencing. We demonstrate the successful use of Illumina deep sequencing technology and subsequent analyses to determine the genetic variants and amino acid substitutions in both treatment-naïve (patient 1) and treatment-experienced (patient 7) isolates from HCV-infected patients. As a result, almost the full nucleotide sequence of HCV was detectable for patients 1 and 7. The reads were mapped to the HCV reference sequence. The coverage was 99.8% and the average depth was 69.5× for patient 7, with values of 99.4% (coverage) and 51.1× (average depth) for patient 1. In patient 7, amino acid (aa) 70 in the core region showed arginine, with methionine at aa 91, by Sanger sequencing. Major variants showed the same amino acid sequence, but minor variants were detectable in 18% (6/34 sequences) of sequences, with replacement of methionine by leucine at aa 91. In NS3, 8 amino acid positions showed mixed variants (T72T/I, K213K/R, G237G/S, P264P/S/A, S297S/A, A358A/T, S457S/C, and I615I/M) in patient 7. In patient 1, 3 amino acid positions showed mixed variants (L14L/F/V, S61S/A, and I586T/I). In conclusion, deep sequencing technologies are powerful tools for obtaining more profound insight into the dynamics of variants in the HCV quasispecies in human serum.

epatitis C virus (HCV) is a positive-strand enveloped RNA virus of approximately 9,600 nucleotide (nt) bases, consisting of a single open reading frame and two untranslated regions, and belongs to the genus *Hepacivirus* within the family *Flaviviridae* (6). The single open reading frame encodes a polyprotein of 3,011 amino acids (aa) that is cleaved by viral and cellular proteases into 10 different proteins. The three structural proteins, which constitute the viral particle, include the core protein and the envelope glycoproteins E1 and E2. Two regions in E2, known as hypervariable regions 1 and 2, are reported to have extreme sequence variability. The seven nonstructural components include the p7 polypeptide, the NS2-3 protease, the NS3 serine protease and RNA helicase, the NS4A polypeptide, the NA4B and NS5A proteins, and the NS5B RNA-dependent RNA polymerase (RdRp) (29). At both ends of the open reading frame lie the 5'- and 3'-untranslated regions (5'-UTR and 3'-UTR). The nucleotide sequence of the 5'-UTR is relatively well conserved among different HCV genotypes. The HCV 5'-UTR contains an internal ribosome entry site (IRES) that directs the cap-independent initiation of virus translation and forms on four characteristic stem-loop structures (17, 18). HCV displays very high genetic variability both in populations and within infected individuals, where it exists as a cluster of closely related but distinct variants, termed "quasispecies," as occurs in many other RNA viruses with a polymerase enzyme lacking proofreading ability (6, 8, 26).

Current standard treatment of chronic HCV infection is based on the combination of pegylated alpha interferon (peg-IFN-α) and ribavirin (RBV). However, patients with a high load of genotype 1b virus ($>1 \times 10^5$ log IU/ml) do not achieve high sustained virological response (SVR) rates ($<50\%$), even when the most effective combination treatment (IFN plus RBV) is administered for 48 weeks (14, 25). Some investigations concerning therapeutic prediction based on virological features revealed that substitutions of arginine for glutamine at amino acid (aa) 70 and/or leu-

cine for methionine at aa 91 in the core region are independent and significant factors associated with SVR or that patients whose viruses have more than 4 amino acid changes in the NS5A interferon sensitivity-determining region (ISDR) (aa 2209 to 2248) have high responses to IFN therapy compared to those for patients with HCV-J (mutant type), whereas patients whose viruses have no amino acid changes (wild type) or 1 to 3 amino acid changes (intermediate type) have low responses (1, 2, 9, 10).

Recently, direct-acting antiviral (DAA) molecules active on HCV, such as NS3/4A protease inhibitors, nucleoside/nucleotide analogue inhibitors of RdRp, nonnucleoside inhibitors of RdRp, and NS5A inhibitors, have been developed. These DAA molecules, either alone or in combination with peg-IFN plus RBV, were recently described as showing large antiviral effects (15, 21). However, the problem that we have to consider next is viral resistance to DAAs due to the selection of viral variants that contain amino acid substitutions altering the drug target and rendering virus less susceptible to the drug's inhibitory activity (35). Additionally, drug-resistant variants already preexist as minor populations within a patient's quasispecies. Drug exposure intensively inhibits replication of the drug-sensitive viral population, and the resistant variants gradually predominate in the HCV population (7). In the future, to determine the most appropriate treatment for HCV

patients, analysis of the nucleotide or amino acid sequence of HCV will become important.

Initial attempts to identify the HCV genome sequence relied on Sanger sequencing and the use of PCR primers targeting relatively conserved regions, methods that would likely fail if the virus had more variants (32–34). In recent years, new technologies have been developed that are able to sequence viruses from environmental samples without using specific primers, cloning, and re-sorting by recombinant DNA techniques and thus can obtain the sequence information for the complete virome in an unbiased way. Metagenomic approaches such as deep sequencing have proven increasingly successful at identifying variants or mutations of the nucleotide sequence (23, 42, 45).

Here we demonstrate the successful use of Illumina deep sequencing technology and subsequent analyses to determine the genetic variants and amino acid substitutions of both treatment-naïve (patient 1) and treatment-experienced (IFN) (patient 7) isolates of HCV without using specific HCV primers.

MATERIALS AND METHODS

Patients. Two patients with chronic hepatitis C virus infection with genotype 1b virus and one healthy control were enrolled in this study. Each serum sample was collected before treatment with peg-IFN-α and RBV and was stored at −20°C until testing. In the laboratory data, the HCV load was 6.8 log IU/ml for patient 1, who was treatment naïve, and 7.0 log IU/ml for patient 7, who was treated with IFN-α2b and RBV for 6 months in 2002, but with no treatment effect (Cobas TaqMan HCV test; Roche Molecular Systems, Pleasanton, CA). More clinical information is described in Table 1.

Sanger sequencing in the core region and NS5A ISDR. Total RNA was extracted from 100-μl serum samples by use of a MagMAX viral RNA isolation kit (Ambion, Austin, TX), and the RNA preparation thus obtained was subjected to cDNA synthesis with reverse transcriptase (SuperScript III RNase H⁻ reverse transcriptase; Invitrogen) and to PCR amplification using Prime Star HS DNA polymerase (TaKaRa Bio, Shiga, Japan) with nested primers derived from the core region and the NS5A ISDR of the HCV genome. Nested PCR amplification of the core region of the HCV genome was carried out with primers C008 (sense; 5′-AAC CTC AAA GAA AAA CCA AAC G-3′) and C011 (antisense; 5′-CAT GGG GTA CAT YCC GCT YG-3′) in the first round, for 35 cycles (98°C for 10 s, 55°C for 15 s, and 72°C for 1 min, with an additional 7 min in the last cycle), and with primers C009 (sense; 5′-CCA CAG GAC GTY AAG TTC CC-3′) and C010 (antisense; 5′-AGG GTA TCG ATG ACC TTA CC-3′) in the second round, for 25 cycles. Nested primers derived from the NS5A ISDR of the HCV genome were designed to amplify a 188-bp product, using primers C004 (sense; 5′-ATG CCC ATG CCA GGT TCC AG-3′) and C005 (antisense; 5′-AGC TCC GCC AAG GCA GAA GA-3′) in the first round and primers C006 (sense; 5′-ACC GGA TGT GGC AGT GCT CA-3′) and C007 (antisense; 5′-GTA ATC CGG GCG TGC CCA TA-3′) in the second round. The PCR products were sequenced directly on both strands by use of a BigDye Terminator, version 3.1, cycle sequencing kit on an ABI Prism 3100 genetic analyzer (Applied Biosystems, Foster City, CA). Sequence analysis was performed using Genetyx-Mac ver. 12.2.6 (Genetyx Corp., Tokyo, Japan) and ODEN (version 1.1.1) from the DNA Data Bank of Japan (National Institute of Genetics, Mishima, Japan) (19).

Library preparation and Illumina sequencing. Total RNA was extracted from 800 μl of serum by use of a MagMAX viral RNA isolation kit (Ambion) according to the manufacturer's protocol, with the slight modification that carrier RNA was not included. A library was prepared from approximately 200 ng of total RNA by use of an mRNA-seq sample prep kit (Illumina, San Diego, CA). The quality of the library was evaluated with Bioanalyzer (Agilent, Santa Clara, CA). Before deep sequencing, we confirmed the presence of the HCV genome in the libraries by conducting quantitative PCR with StepOnePlus (Applied Biosystems), using SYBR Ex

TABLE 1 Clinical data for patients enrolled in this study[a]

Patient (storage date of sample)	Sex	Age (yr)	Diagnosis	HCV RNA load (log IU/ml)	HCV genotype	Past treatment (period)	Therapeutic effect	Core aa 70	Core aa 91	No. of aa substitutions in NS5A ISDR
1 (October 2008)	Male	43	Chronic hepatitis C	6.8	1b	None	NA	Wild type	Wild type	0
7 (May 2010)	Male	57	Chronic hepatitis C	7.0	1b	IFN-α2b plus RBV (March–September 2002)	Nontherapeutic	Wild type	Mutant	0
9 (January 2011)	Female	64	Control	NA	NA	NA	NA	NA	NA	NA

[a] Abbreviations: aa, amino acid; IFN, interferon; NA, not applicable; RBV, ribavirin. All patients were negative for hepatitis B surface antigen (HBsAg) and hepatitis B surface antibody (HBsAb).
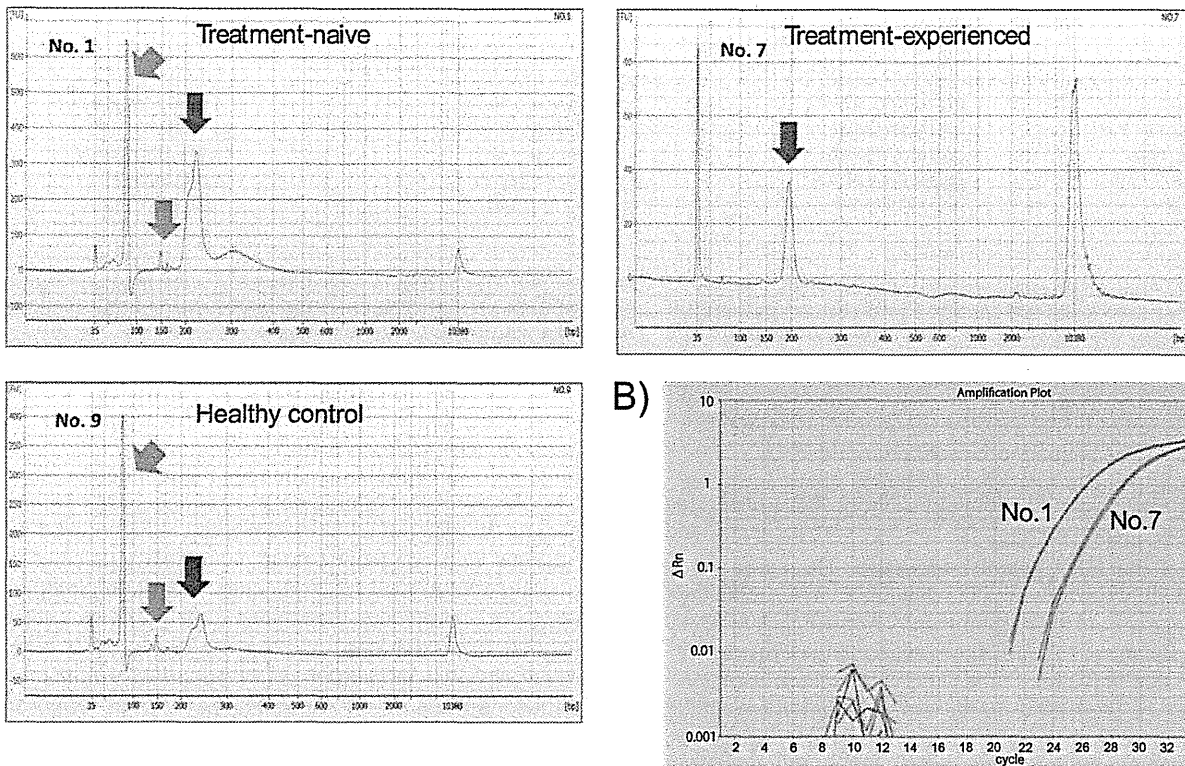
— 1692 —

FIG 1 Evaluation of the quality of libraries. (A) The library was well refined for patient 7, but the primer and adaptor dimers were mixed in the libraries of patients 1 and 9, obtained using Bioanalyzer (Agilent). The horizontal axis shows the DNA size, and the vertical axis shows the quantity of DNA. The blue arrows indicate the desired products, and the red arrows indicate the primer or adaptor dimers. The peaks of the wave at 35 bp and 10,380 bp express the marker. (B) Amplification plots for patients 1 (treatment naïve) and 7 (treatment experienced), showing the presence of the HCV genome in the libraries by quantitative PCR with StepOnePlus (Applied Biosystems).

Taq premix (TaKaRa, Shiga, Japan) and the specific primers C112 (sense; 5′-GCW GTS CAR TGG ATG AAC CG-3′) and C113 (antisense; 5′-GCT YTC MGG CAC RTA GTG CG-3′), derived from the 81-bp region encoding HCV NS4B, and then loaded each sample into two or three lanes of a flow cell. Libraries were clonally amplified on the flow cell and sequenced on an Illumina IIx genome analyzer (SCS 2.8 software; Illumina, San Diego, CA), with a 76-mer single end sequence. Image analysis and base calling were performed using RTA 1.8 software.

Analysis. Seventy-six-mer single-end reads were classified by strict bar codes, split into individual reads, and stripped of any remaining primer sequences by using CLC Genomics Workbench (4.6) (http://www.clcbio .co.jp). Sequence reads aligned to the human genome by hg19 (http: //hgdownload.cse.ucsc.edu/goldenPath/hg19/bigZips/chromFa.tar.gz), GenBank (http://hgdownload.cse.ucsc.edu/goldenPath/hg19/bigZips /mrna.fa.gz), RefSeq (http://hgdownload.cse.ucsc.edu/goldenPath /hg19/bigZips/refMrna.fa.gz), and Ensembl (ftp://ftp.ensembl.org/pub /release62/fasta/homo_sapiens/cdna/Homo_sapiens.GRCh37.62.cdna .all.fa.gz and ftp://ftp.ensembl.org/pub/release62/fasta/homo_sapiens/ ncrna/Homo_sapiens.GRCh37.62.ncrna.fa.gz) were removed in the first mapping analysis of the human genome. Sequence reads not of human origin were aligned with 970 reference HCV sequences registered at the Hepatitis Virus Database server (http://s2as02.genes.nig.ac.jp/index .html) by use of BWA (0.5.9-r16), allowing mismatches within 5 to 10 nucleotide bases (24). The reads could be defined as being of HCV origin by identification with reference to the HCV sequences, allowing mismatches within 10 nucleotide bases. Duplicate reads were completely excluded to avoid sequence bias, using Samtools (0.1.16) (24). Additionally,

the variants compared with HCV-J were identified by Samtools. The result of the analysis was displayed using Integrative Genomics Viewer (IGV; 2.0.3) (36).

Ethics statement. Written informed consent was obtained from each individual, and the study for detecting host genomes was approved by the Ethics Committee of the Tohoku University School of Medicine (2010-404).

RESULTS

Evaluation of the quality of the libraries. We conducted deep sequencing analysis for two patients (patient 1 [treatment naïve] and patient 7 [treatment experienced, with IFN]) who had been infected with chronic hepatitis C virus of genotype 1b, as well as one healthy control (patient 9) (Table 1). Since there is only a small quantity of circulating RNAs, including those of viral origin, in serum, it was important to evaluate the quality of the libraries. The library for patient 7 showed good quality using an Agilent bioanalyzer, but the primer and adaptor dimers were mixed in the libraries of patients 1 and 9 (Fig. 1A). Before deep sequencing, we evaluated whether the HCV genome was included in the libraries, and the amplification plots for quantitative PCR showed that the HCV genome could be detected in the libraries from both patients 1 and 7 with the specific primers C112 and C113, derived from the NS4B region (Fig. 1B).

Distribution of free RNA in human serum. To characterize the metagenomics of HCV infection in humans, we analyzed

— 1693 —

TABLE 2 Distribution of viral reads in human serum

Sample	No. (%) of reads		
	Patient 1 (treatment naïve)	Patient 7 (treatment experienced)	Patient 9 (healthy control)
Total reads	27,717,487 (100.00)	94,151,356 (100.00)	15,032,130 (100.00)
Adaptor and primer reads	6,502,508 (23.46)	28,605,006 (30.38)	5,713,994 (38.01)
Modified total reads	21,214,979 (76.54)	65,546,350 (69.62)	9,318,136 (61.99)
Reads of human origin	19,761,560 (71.30)	58,446,916 (62.08)	8,660,143 (57.61)
Unknown reads	1,453,419 (5.24)	7,099,434 (7.54)	657,993 (4.38)

the samples by single-end deep sequencing on three lanes for patient 7 and on two lanes for patient 1 and control patient 9, using an Illumina IIx genome analyzer. After trimming the reads to exclude ambiguous nucleotides, primers, or adaptor sequences, 96,079,465 high-quality 76-bp reads were subjected to analysis. From the initial set of reads, a total of 86,868,619 reads were able to be aligned to human genomic DNA.

We then mapped the remaining 9,210,846 reads, including 1,453,419 reads for patient 1, 7,099,434 reads for patient 7, and 657,993 reads for patient 9 (Table 2).

Mapping of the HCV genome sequence. The reads were aligned to 970 HCV genome sequences by using BWA, allowing mismatches within 5 to 10 nucleotide bases. Accordingly, MD5-1 (GenBank accession no. AF165053) was expected to be the closest HCV strain to that in patient 1, and MD2-2 (GenBank accession no. AF165048) was expected to be the closest to that in patient 7. The reads obtained from healthy subject 9 were not aligned to MD5-1 or MD2-2, allowing mismatches within 10 nucleotide bases (see the supplemental material). Whereas some strains, for example, HC-J4, HCV-KT9, and HC-J6, could be mapped to the reads from healthy subject 9, all of the reads were aligned at the 3'-UTR of the U-rich region, and we could not evaluate whether they were of HCV origin. Therefore, we constituted the HCV genome sequences of patients 1 and 7 without the 3'-UTR. In this alignment, the duplicate reads were completely excluded. For patient 1, 6,303 reads were mapped on MD5-1, allowing for 10 mismatched nucleotide bases. The coverage was 99.4%, and the aver-

age depth was 51.1× (Fig. 2). For patient 7, 8,583 reads could be identified with MD2-2. The coverage was 99.8%, and the average sequencing depth was 69.5× (Fig. 2).

Notably, the genome sequence could not be obtained for only 8 nt in the 5'-UTR and 52 nt in the core region for patient 1 and for 18 nt in the E2 region for patient 7.

Amino acid substitutions in the core region and the NS5A ISDR. To identify potential mutations at key sites in the genome that mediate the effect of IFN-based therapy, we compared the HCV genome obtained from patient 7 with HCV-J, which is known as the prototypical HCV 1b strain and whose complete genomic sequence has been determined (20). A previous study reported that there were substitutions of aa 70 and/or 91 in the core region and that the number of substitutions within three bases in the region of aa 2209 to 2248 (NS5A ISDR) might be associated with resistance to IFN-based therapy (1, 2, 9, 10). Position 70 in the core region showed arginine, with methionine at aa 91, by Sanger sequencing. In deep sequencing, major variants showed the same amino acid sequence, but minor variants were detectable in 18% (6/34 sequences) of sequences, with replacement of methionine by leucine at aa 91 (Fig. 3A). In the NS5A ISDR, no substitution was indicated for major variants, the same as in direct sequencing by Sanger sequencing, but 16% (14/89 sequences) of sequences showed minor variant replacements of aspartic acid by valine at aa 2220 (Fig. 3B). We validated that more than 10% of the detected variants were effective. For patient 1, core aa 70 (arginine), core aa 91 (leucine), and the number of
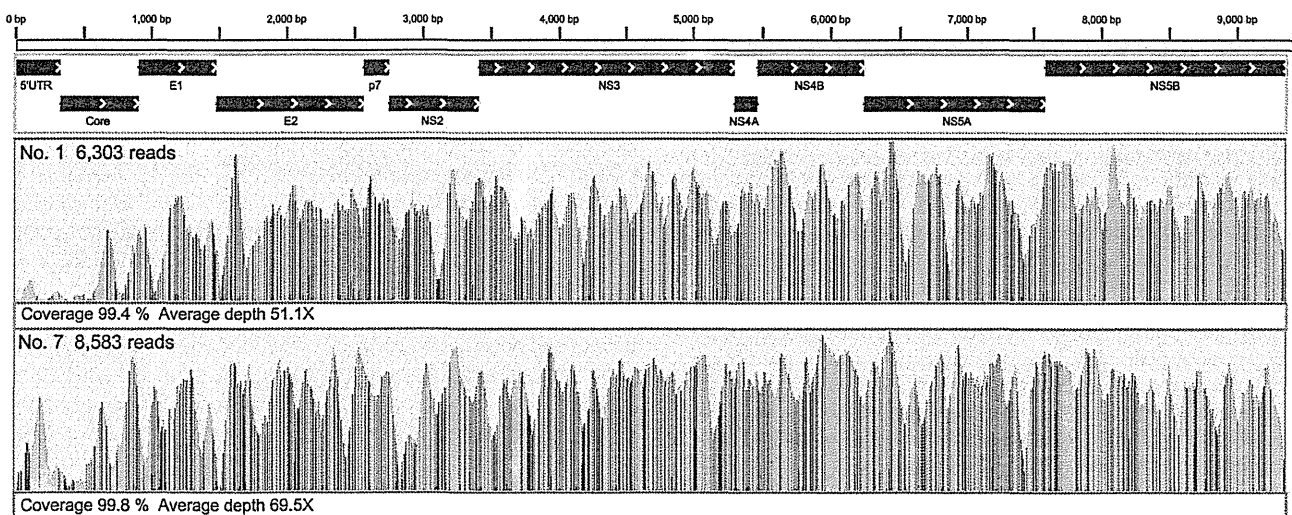
FIG 2 Mapping to the HCV reference genome. For patient 1, 6,303 reads were mapped to MD5-1. The coverage was 99.4%, and the average depth was 51.1×. For patient 7, 8,583 reads were aligned to MD2-2. The coverage was 99.8%, and the average depth was 69.5%.

— 1694 —

A) Core aa. 70 and aa. 91

		Core aa. 70	Core aa. 91
Sanger sequencing		R	M
		Wild	Mutation
Deep sequencing		R (100 %)	M (72 %)/L (18 %)
		Wild	Mutation/Wild

B) NS5A-ISDR

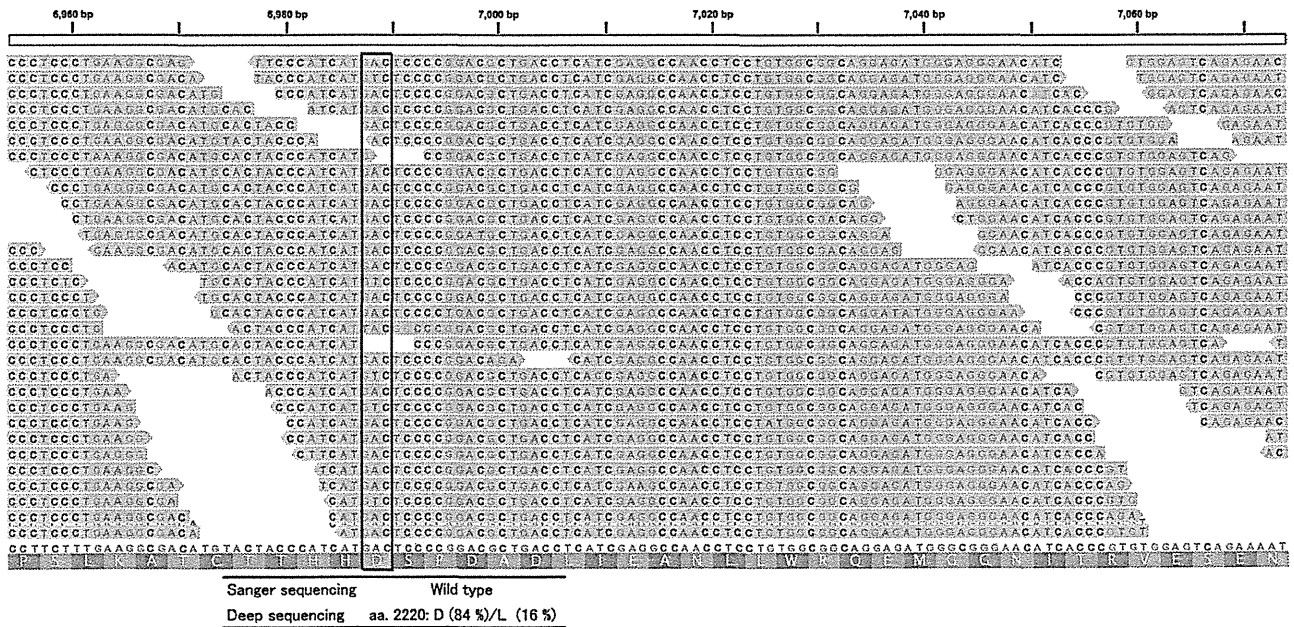| Sanger sequencing	Wild type
Deep sequencing	aa. 2220: D (84 %)/L (16 %)
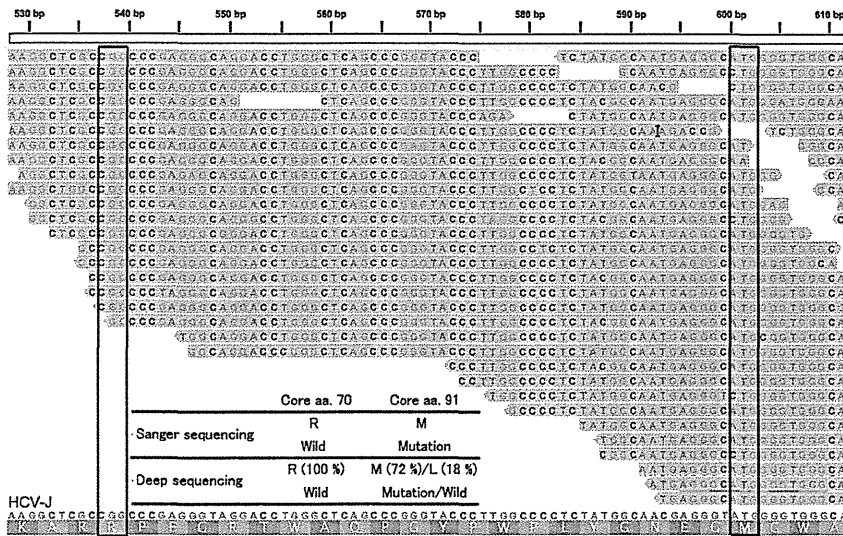
FIG 3 Amino acid substitutions of aa 70 and 91 in the core region (A) and aa 2209 to 2248 of the NS5A ISDR (B). Mutations in these regions were reported to affect the outcome of IFN-based therapies for chronic hepatitis C patients. The lower two lines show the nucleotide sequence and amino acid sequence of HCV-J. Amino acid abbreviations: F, phenylalanine; S, serine; Y, tyrosine; C, cysteine; W, tryptophan; L, leucine; P, proline; H, histidine; Q, glutamine; R, arginine; I, isoleucine; M, methionine; T, threonine; N, asparagine; K, lysine; V, valine; A, alanine; D, aspartic acid; E, glutamic acid; G, glycine.

NS5A ISDR mutations (zero) were the same as those by Sanger sequencing.

Amino acid substitutions in NS3 and NS5B. The recent development of DAA molecules, such as protease inhibitors and polymerase inhibitors, has raised the concern that resistance may weaken the effects of DAA-based therapy (35). It is necessary to obtain the amino acid sequences of NS3 or NS5B variants bearing substitutions which alter the target of the drug. In NS3 in the virus from patient 7, 26 amino acids were changed in comparison with

the prototype strain HCV-J. Eight amino acids showed mixed variants, with T72T/I (57 variants [75%]/21 variants [27%]), K213K/R (18 variants [26%]/52 variants [74%]), G237G/S (41 variants [46%]/49 variants [54%]), P264P/S/A (20 variants [42%]/19 variants [40%]/9 variants [19%]), S297S/A (63 variants [81%]/15 variants [19%]), A358A/T (20 variants [21%]/75 variants [79%]), S457S/C (56 variants [64%]/32 variants [36%]), and I615I/M (42 variants [46%]/49 variants [54%]) substitutions (Table 3). For NS5B, the full amino acid sequence was observed, and

— 1695 —

TABLE 3 Amino acid substitutions compared with HCV-J in NS3 and NS5B from viruses of patients 1 and 7

Protein and patient	Nucleotide position	Amino acid position	Prototype amino acid	Nucleotide sequence[a]	Amino acid substitution[b]
NS3					
Patient 1	3426	7	S	gCC	A
	3447	14	L	(C/t/g)TT	L/F/V (67 [89]/6 [8]/2 [3])
	3495	30	D	GAg	E
	3513	36	L	gTt	V
	3588	61	S	(T/g)CG	S/A (48 [71]/20 [29])
	3591	62	K	AgG	R
	3618	71	I	gTC	V
	3645	80	Q	CtG	L
	3663	86	P	CaG	Q
	3747	114	V	aTc	I
	3801	132	I	gTC	V
	3855	150	V	GcT	A
	3915	170	I	gT(A/g)	V
	4149	248	I	gTC	V
	4152	249	E	GAc	D
	4191	262	G	aGC	S
	4194	263	G	Gct	A
	4218	271	C	gGC	G
	4302	299	T	tCC	S
	4392	329	I	gTC	V
	4479	358	A	aaC	N
	4551	382	T	tCg	S
	4554	382	G	GcC	A
	4563	386	L	gTC	V
	4659	418	F	TaT	Y
	4758	451	L	gTG	V
	4782	459	A	tCG	S
	4815	470	S	gGg	G
	4935	510	S	aCa	T
	5007	534	S	gGC	G
	5076	557	L	tTC	F
	5163	586	I	A(T/c)A	I/T (4 [12]/30 [88])
	5232	609	V	aTC	I
	5268	621	A	aCA	T
Patient 7	3495	30	D	GAg	E
	3513	36	L	gTt	V
	3531	42	S	aCT	T
	3549	48	V	aTC	I
	3621	72	T	A(C/t)C	T/I (57 [73]/21 [27])
	3663	86	P	CaG	Q
	3672	89	P	tCC	S
	3687	94	M	tTG	L
	3747	114	V	aTc	I
	3801	132	I	gTC	V
	3855	150	V	GcT	A
	3915	170	I	gTA	V
	4044	213	K	A(A/g)g	K/R (18 [26]/52 [74])
	4116	237	G	(G/a)G(C/t)	G/S (41 [46]/49 [54])
	4149	248	I	gTt	V
	4152	249	E	Gac	D
	4194	263	G	Gct	A
	4197	264	P	(C/t/g)CC	P/S/A (20 [42]/19 [40]/9 [19])
	4218	271	C	gGC	G
	4296	297	S	(T/g)CG	S/A (63 [81]/15 [19])
	4302	299	T	tCC	S
	4479	358	A	(G/a)CC	A/T (20 [21]/74 [79])
	4542	379	A	tCA	S
	4551	382	T	tCA	S
	4554	383	G	acC	T
	4563	386	L	aTC	I
	4659	418	F	TaT	Y
	4758	451	L	gTG	V
	4776	457	S	T(C/g)(G/t)	S/C (56 [64]/32 [36])
	4782	459	A	tCg/a	S
	4815	470	S	gcg	A
	5076	557	L	tTC	F
	5172	589	K	AgG	R
	5250	615	I	AT(A/g)	I/M (42 [46]/49 [54])
	5259	618	Y	TtC	F

(Continued on following page)

— 1696 —

TABLE 3 (Continued)

Protein and patient	Nucleotide position	Amino acid position	Prototype amino acid	Nucleotide sequence[a]	Amino acid substitution[b]
NS5B					
Patient 1	7659	25	P	gCG	A
	7689	35	S	Aac	N
	7701	39	S	gCC	A
	7725	47	L	CaG	Q
	7827	81	R	Aaa	K
	7839	85	I	gTA	V
	7878	98	K	AgA	R
	7914	110	S	AaC	N
	7932	116	V	aTt	I
	7944	120	R	CaC	H
	7956	124	E	aAG	K
	7989	135	D	aAc	N
	8025	147	V	aTt	I
	8151	189	P	tCC	S
	8205	207	T	gCC	A
	8223	213	C	aaC	N
	8238	218	S	gCA	A
	8289	235	T	gtT	V
	8370	262	V	aTt	I
	8484	300	T	tCT	S
	8532	316	N	tgC	C
	8589	335	A	aaC	N
	8598	338	A	GtC	V
	8784	400	V	GcT	A
	8937	451	C	acT	T
	8976	464	E	cAg	Q
	9153	523	K	Aga	R
	9177	531	K	AgG	R
	9252	556	N	AgC	S
	9276	564	L	gTG	V
	9306	574	L	TgG	W
Patient 7	7599	5	T	tCA	S
	7689	35	S	Aa(c/t)	N
	7701	39	S	gCC	A
	7725	47	L	Caa	Q
	7827	81	R	Aaa	K
	7839	85	I	gTg	V
	7878	98	K	AgA	R
	7914	110	S	AaC	N
	7926	114	R	Aaa	K
	7956	124	E	aAG	K
	8151	189	P	tCC	S
	8205	207	T	gCC	A
	8223	213	C	acC	T
	8238	218	S	gCA	A
	8277	231	N	AgT	S
	8289	235	T	gtT	V
	8298	238	S	gCA	A
	8370	262	V	aTC	I
	8484	300	T	tCT	S
	8532	316	N	tgC	C
	8589	335	A	agC	S
	8784	400	V	GcT	A
	8937	451	C	acT	T
	8940	452	Y	cAC	H
	8946	454	I	gTT	V
	8976	464	E	cAA	Q
	9177	531	K	AgG	R
	9213	543	S	TtC	F
	9231	549	G	aaC	N
	9252	556	N	AgC	S
	9306	574	L	TgG	W

[a] Uppercase letters indicate prototype nucleotides, and lowercase letters indicate mutations.
[b] The numbers and percentages of amino acid bases are displayed in parentheses and brackets, respectively.

— 1697 —

31 amino acids were altered in comparison with HCV-J. No mixed variants were seen (Table 3). With patient 1, full amino acid sequences were detected for NS3 and NS5B. Compared with HCV-J, 31 amino acids were altered in NS3, and 3 amino acids showed mixed variants, with L14L/F/V (67 variants [89%]/6 variants [8%]/2 variants [3%]), S61S/A (48 variants [71%]/20 variants [29%]), and I586I/T (4 variants [12%]/30 variants [88%]) substitutions (Table 3). In NS5B, 31 amino acids were converted (Table 3). Note that more than 10% of the minor variants were confirmed as effective.

DISCUSSION

In this study, we attempted to detect the HCV genome directly in human serum without using specific primers and succeeded in determining and certifying nearly the full genome sequence and a high genetic diversity by using deep Illumina sequencing. HCV has already been reported to be a highly variable virus with a quasispecies distribution, large viral populations, and very rapid turnover in individual patients (6, 26). Previous studies using metagenomic sequencing of other viruses from human clinical samples mostly employed pyrosequencing (11, 12, 23, 30, 46). The longer reads from pyrosequencing (250 to 450 bp) facilitate the assembly of individual reads into contigs, which facilitates the classification of the sequence data by homology-based BLAST alignment. In contrast to metagenomic analysis using pyrosequencing, Illumina short-read sequencing enables a greater depth (by an order of magnitude) that is reflected in a very low detection limit. A recent report revealed that viral transcripts could be found at frequencies of <1 in 1,000,000 (28). However, because of short reads, de novo assembly without any reference is difficult to conduct, so it is not suitable for discovering an unknown viral genome. However, it seems quite useful for resequencing or detection of variants of known viruses for which abundant nucleotide sequence data have already been reported.

We defined the Illumina 76-mer reads as being of HCV origin by relying on the 970 HCV genome sequences in this study. HCV shows considerable genetic diversity and has been classified into 11 genogroups or 6 groups by the core, E1, or NS5B region, with nucleotide divergence. Only about 75% similarity was shown in the variable region, even for the same group (38, 39, 44). The reads were aligned to each of the 970 HCV sequences, allowing mismatches within 10 nucleotide bases. Under these conditions, we could not map the reads of HCV isolates without the 3'-UTR region for patient 9, who had not been infected with HCV. This is because the 3'-UTR has a U-rich region, and it is impossible to decide the reads of HCV origin with specificity. Therefore, we aligned the reads to the full HCV sequence without the 3'-UTR for patients 1 and 7.

Many variants with different nucleotide bases, known as quasispecies, were detected in both patients 1 and 7. Taking a close look at the mixed variants with amino acid substitutions in NS3, patient 7 showed 8 variants, while there were only 3 variants in patient 1. Recent studies reported that HCV genomic sequences in treatment relapsers displayed significantly more mutations than those in nonresponders. HCV sequence analysis of a 4-year post-antiviral-therapy follow-up revealed that the vast majority of mutations selected during the therapy phase were maintained in the relapsers, while very few new mutations arose during the 4-year posttherapy span (5,

47). Based on the experiments mentioned above, treatment with IFN may lead to the emergence of mutations. Deep sequencing is considered a useful tool for detecting viral variants and determining the mutational rate without cloning.

Although there were only a few detected reads of HCV origin obtained from serum, metagenomic analysis could be conducted with the enormous data sets generated by deep sequencing. Consequently, almost the full genome sequence of HCV was demonstrated by using computational analysis of sequential alignments of individual reads, with average depths of 51.1× and 69.5×. However, the regions for which we could not obtain the sequence were 8 nt in the 5'-UTR and 52 nt in the core region for patient 1 and 18 nt in the E2 region for patient 7. Since the 5'-UTR forms on characteristic stem-loop structures, Sanger sequencing is generally difficult (31). Similarly, even deep Illumina sequencing appears to be difficult. Since the E2 region, known as a hypervariable region, is reported to have extreme sequence variability, it was predicted that there would be too many mismatches with the reference HCV genome and that the reads could not be mapped by this analysis. Analysis of this hypervariable region will require further work.

Comparing the qualities of the libraries from patients 1 and 7, that of patient 7 was well refined; hence, the quality of the library is important for gaining large amounts of expected reads. However, a lot of duplicate reads were found for patient 7, and in fact, to analyze the full sequence of HCV, it is considered sufficient to use two lanes for Illumina sequencing.

Amino acid substitutions of core aa 70 and 91 and within the NS5A ISDR, as well as genetic polymorphisms in the host IL28B gene, encoding IFN-λ-3 on chromosome 19, affect the outcome of interferon-based therapies for chronic hepatitis C patients (1, 2, 9, 10, 16, 40, 43). Even if only the amino acid substitution of a major variant were assumed, an accurate therapeutic effect would be impossible to predict. The proportion of minor variants may change the therapeutic effect, and variants cannot be detected only by direct sequencing using Sanger sequencing. In fact, patient 7 showed a methionine at aa 91 in the core region and no substitution in the NS5A ISDR by direct Sanger sequencing, but deep sequencing indicated minor variants (at aa 91 in the core region [18% of sequences] and in the NS5A ISDR [15% of sequences]).

Recently, DAA molecules have been developed for HCV therapies, and these drugs may lead to the selection of resistant viruses if administered alone. The first-generation NS3/4A inhibitors are telaprevir and boceprevir, and most of the reported clinical data on drug resistance were obtained from patients treated with telaprevir. As an illustration, based on in vitro studies, telaprevir resistance related to amino acid substitutions V36A/M/C, T54A/S, R155K/T/Q, A155V/T, and A156T has been reported (4, 22, 37). Substitutions that generated boceprevir resistance included those detected in a patient treated with telaprevir, plus V170A/T and V55A substitutions (13, 41). Of the nonnucleoside inhibitors of RdRp displaying inhibitory activities against the RdRp enzyme at NS5B, few have been reported in the in vivo resistance data (27). This is because studies of antiviral efficacy are generally limited to 3 to 5 days. Yet, for example, the S282T substitution has been reported to confer a loss of in vitro sensitivity to nucleoside/nucleotide analogue inhibitors (3). In the future, the triple combination of peg-IFN-α, RBV, and a protease inhibitor or several combina-

− 1698 −

tions of DAAs will soon become the standard therapy for treatment-naïve and treatment-experienced patients with HCV genotype 1. In this study, though neither patient 1 nor patient 7 showed drug-resistant variants, it would be very important for the selection of therapy to identify resistant or minor variants prior to treatment. Additionally, when treatment has failed, it is necessary to consider viral factors as a cause.

In conclusion, deep sequencing technologies are a powerful tool for obtaining more profound insight into the dynamics of variants in the HCV quasispecies in human serum. Although the cost of deep sequencing is still much greater than the reagent costs for Sanger sequencing, it is still attractive in clinical medicine because deep sequencing is able to generate much more information on the viral genome sequences in internal organs. The cost will decrease in the future as the technology of deep sequencing develops. As DAA combination treatment of HCV infection is developed, obtaining sequence information on variants in individual cases by use of deep sequencing will be feasible for determining optimal antiviral treatment.

ACKNOWLEDGMENTS

REFERENCES

1. Akuta N, et al. 2007. Prediction of response to pegylated interferon and ribavirin in hepatitis C by polymorphisms in the viral core protein and very early dynamics of viremia. Intervirology 50:361–368.
2. Akuta N, et al. 2005. Association of amino acid substitution pattern in core protein of hepatitis C virus genotype 1b high viral load and non-virological response to interferon-ribavirin combination therapy. Intervirology 48:372–380.
3. Ali S, et al. 2008. Selected replicon variants with low-level in vitro resistance to the hepatitis C virus NS5B polymerase inhibitor PSI-6130 lack cross-resistance with R1479. Antimicrob. Agents Chemother. 52:4356–4369.
4. Barbotte L, et al. 2010. Characterization of V36C, a novel amino acid substitution conferring hepatitis C virus (HCV) resistance to telaprevir, a potent peptidomimetic inhibitor of HCV protease. Antimicrob. Agents Chemother. 54:2681–2683.
5. Cannon NA, Donlin MJ, Fan X, Aurora R, Tavis JE. 2008. Hepatitis C virus diversity and evolution in the full open-reading frame during antiviral therapy. PLoS One 3:e2123.
6. Choo QL, et al. 1991. Genetic organization and diversity of the hepatitis C virus. Proc. Natl. Acad. Sci. U. S. A. 88:2451–2455.
7. Clavel F, Hance AJ. 2004. HIV drug resistance. N. Engl. J. Med. 350:1023–1035.
8. Domingo E, et al. 1985. The quasispecies (extremely heterogeneous) nature of viral RNA genome populations: biological relevance—a review. Gene 40:1–8.
9. Enomoto N, et al. 1995. Comparison of full-length sequences of interferon-sensitive and resistant hepatitis C virus 1b. Sensitivity to interferon is conferred by amino acid substitutions in the NS5A region. J. Clin. Invest. 96:224–230.
10. Enomoto N, et al. 1996. Mutations in the nonstructural protein 5A gene and response to interferon in patients with chronic hepatitis C virus 1b infection. N. Engl. J. Med. 334:77–81.
11. Feng H, Shuda M, Chang Y, Moore PS. 2008. Clonal integration of a polyomavirus in human Merkel cell carcinoma. Science 319:1096–1100.
12. Finkbeiner SR, et al. 2009. Identification of a novel astrovirus (astrovirus VA1) associated with an outbreak of acute gastroenteritis. J. Virol. 83:10836–10839.
13. Flint M, et al. 2009. Selection and characterization of hepatitis C virus replicons dually resistant to the polymerase and protease inhibitors HCV-796 and boceprevir (SCH 503034). Antimicrob. Agents Chemother. 53:401–411.
14. Fried MW, et al. 2002. Peginterferon alfa-2a plus ribavirin for chronic hepatitis C virus infection. N. Engl. J. Med. 347:975–982.
15. Gao M, et al. 2010. Chemical genetics strategy identifies an HCV NS5A inhibitor with a potent clinical effect. Nature 465:96–100.
16. Ge D, et al. 2009. Genetic variation in IL28B predicts hepatitis C treatment-induced viral clearance. Nature 461:399–401.
17. Honda M, Beard MR, Ping LH, Lemon SM. 1999. A phylogenetically conserved stem-loop structure at the 5' border of the internal ribosome entry site of hepatitis C virus is required for cap-independent viral translation. J. Virol. 73:1165–1174.
18. Honda M, et al. 1996. Structural requirements for initiation of translation by internal ribosome entry within genome-length hepatitis C virus RNA. Virology 222:31–42.
19. Ina Y. 1994. ODEN: a program package for molecular evolutionary analysis and database search of DNA and amino acid sequences. Comput. Appl. Biosci. 10:11–12.
20. Kato N, et al. 1990. Molecular cloning of the human hepatitis C virus genome from Japanese patients with non-A, non-B hepatitis. Proc. Natl. Acad. Sci. U. S. A. 87:9524–9528.
21. Kieffer TL, et al. 2007. Telaprevir and pegylated interferon-alpha-2a inhibit wild-type and resistant genotype 1 hepatitis C virus replication in patients. Hepatology 46:631–639.
22. Kwong AD, McNair L, Jacobson I, George S. 2008. Recent progress in the development of selected hepatitis C virus NS3.4A protease and NS5B polymerase inhibitors. Curr. Opin. Pharmacol. 8:522–531.
23. Lataillade M, et al. 2010. Prevalence and clinical significance of HIV drug resistance mutations by ultra-deep sequencing in antiretroviral-naive subjects in the CASTLE study. PLoS One 5:e10952.
24. Li H, et al. 2009. The sequence alignment/map format and SAMtools. Bioinformatics 15:2078–2079.
25. Manns MP, et al. 2001. Peginterferon alfa-2b plus ribavirin compared with interferon alfa-2b plus ribavirin for initial treatment of chronic hepatitis C: a randomised trial. Lancet 358:958–965.
26. Martell M, et al. 1992. Hepatitis C virus (HCV) circulates as a population of different but closely related genomes: quasispecies nature of HCV genome distribution. J. Virol. 66:3225–3229.
27. McCown MF, et al. 2008. The hepatitis C virus replicon presents a higher barrier to resistance to nucleoside analogs than to nonnucleoside polymerase or protease inhibitors. Antimicrob. Agents Chemother. 52:1604–1612.
28. Moore RA, et al. 2011. The sensitivity of massively parallel sequencing for detecting candidate infectious agents associated with human tissue. PLoS One 6:e19838.
29. Moradpour D, Penin F, Rice CM. 2007. Replication of hepatitis C virus. Nat. Rev. Microbiol. 5:453–463.
30. Nakamura S, et al. 2009. Direct metagenomic detection of viral pathogens in nasal and fecal specimens using an unbiased high-throughput sequencing approach. PLoS One 4:e4219.
31. Ninomiya M, Takahashi M, Shimosegawa T, Okamoto H. 2007. Analysis of the entire genomes of fifteen torque teno midi virus variants classifiable into a third group of genus Anellovirus. Arch. Virol. 152:1961–1975.
32. Okamoto H, et al. 1992. Genetic drift of hepatitis C virus during an 8.2-year infection in a chimpanzee: variability and stability. Virology 190:894–899.
33. Okamoto H, et al. 1992. Full-length sequence of a hepatitis C virus genome having poor homology to reported isolates: comparative study of four distinct genotypes. Virology 188:331–341.
34. Okamoto H, et al. 1993. Characterization of the genomic sequence of type V (or 3a) hepatitis C virus isolates and PCR primers for specific detection. J. Gen. Virol. 74:2385–2390.
35. Pawlotsky JM. 2011. Treatment failure and resistance with direct-acting antiviral drugs against hepatitis C virus. Hepatology 53:1742–1751.
36. Robinson JT, et al. 2011. Integrative genomics viewer. Nat. Biotechnol. 29:24–26.
37. Sarrazin C, et al. 2007. Dynamic hepatitis C virus genotypic and phenotypic changes in patients treated with the protease inhibitor telaprevir. Gastroenterology 132:1767–1777.
38. Simmonds P, et al. 1994. Identification of genotypes of hepatitis C virus

— 1699 —

by sequence comparisons in the core, E1 and NS-5 regions. J. Gen. Virol. 75:1053–1061.

39. Smith DB, et al. 1997. The origin of hepatitis C virus genotypes. J. Gen. Virol. 78:321–328.

40. Suppiah V, et al. 2009. IL28B is associated with response to chronic hepatitis C interferon-α and ribavirin therapy. Nat. Genet. 41:1100–1104.

41. Susser S, et al. 2009. Characterization of resistance to the protease inhibitor boceprevir in hepatitis C virus-infected patients. Hepatology 50: 1709–1718.

42. Szpara ML, Parsons L, Enquist LW. 2010. Sequence variability in clinical and laboratory isolates of herpes simplex virus 1 reveals new mutations. J. Virol. 84:5303–5313.

43. Tanaka Y, et al. 2009. Genome-wide association of IL28B with response to pegylated interferon-α and ribavirin therapy for chronic hepatitis C. Nat. Genet. 41:1105–1109.

44. Tokita H, et al. 1996. Hepatitis C virus variants from Jakarta, Indonesia classifiable into novel genotypes in the second (2e and 2f), tenth (10a) and eleventh (11a) genetic groups. J. Gen. Virol. 77:293–301.

45. Verbinnen T, et al. 2010. Tracking the evolution of multiple in vitro hepatitis C virus replicon variants under protease inhibitor selection pressure by 454 deep sequencing. J. Virol. 84:11124–11133.

46. Victoria JG, et al. 2009. Metagenomic analyses of viruses in stool samples from children with acute flaccid paralysis. J. Virol. 83:4642–4651.

47. Xiang X, et al. 2011. Viral sequence evolution in Chinese genotype 1b chronic hepatitis C patients experiencing unsuccessful interferon treatment. Infect. Genet. Evol. 11:382–390.

Sequential immunological analysis of HBV/HCV co-infected patients during Peg-IFN/RBV therapy

Yasuteru Kondo · Yoshiyuki Ueno · Masashi Ninomiya · Keiichi Tamai ·
Yasuhito Tanaka · Jun Inoue · Eiji Kakazu · Koju Kobayashi · Osamu Kimura ·
Masahito Miura · Takeshi Yamamoto · Tomoo Kobayashi · Takehiko Igarashi ·
Tooru Shimosegawa

Abstract

Background The immunopathogenesis of dual chronic infection with hepatitis B virus and hepatitis C virus (HBV/HCV) remains unclear. The in vivo suppressive effects of each virus on the other have been reported. In this study we aimed to analyze the virological and immunological parameters of HBV/HCV coinfected patients during pegylated interferon/ribavirin (Peg-IFN/RBV) therapy.

Methods One patient with high HBV-DNA and high HCV-RNA titers (HBV-high/HCV-high) and 5 patients with low HBV-DNA and high HCV-RNA titers (HBV-low/HCV-high) were enrolled. Twenty patients monoinfected with HBV and 10 patients monoinfected with HCV were enrolled as control subjects.. In vitro cultures of Huh 7 cells with HBV/HCV dual infection were used to analyze the direct interaction of HBV/HCV.

Results Direct interaction of HBV clones and HCV could not be detected in the Huh-7 cells. In the HBV-high/HCV-high-patient, the HCV-RNA level gradually declined and HBV-DNA gradually increased during Peg-IFN/RBV therapy. Activated CD4- and CD8-positive T cells were increased at 1 month of Peg-IFN/RBV-therapy, but HBV-specific IFN-γ-secreting cells were not increased and HBV-specific interleukin (IL)-10 secreting cells were increased. The level of HBV- and HCV-specific IFN-γ-secreting cells in the HBV-high/HCV-high-patient was low in comparison to that in the HBV- or HCV-monoinfected patients. In the HBV-low/HCV-high-patient, HCV-RNA and HBV-DNA rapidly declined during Peg-IFN/RBV therapy. Activated CD4- and CD8-positive T cells were increased, and HBV- and HCV-specific IFN-γ-secreting cells were also increased during Peg-IFN/RBV-therapy.

Conclusion The immunological responses of the HBV-high/HCV-high patient were low in comparison to the responses in HBV and HCV monoinfected patients. Moreover, the response of immune cells in the HBV-high/HCV-high patient during Peg-IFN/RBV therapy was insufficient to suppress HBV and HCV.

Keywords Dual infection · HBV · HCV · Immunopathogenesis

Y. Kondo · Y. Ueno (✉) · M. Ninomiya · K. Tamai ·
J. Inoue · E. Kakazu · O. Kimura · T. Shimosegawa
Division of Gastroenterology, Tohoku University Graduate
School of Medicine, 1-1 Seiryo, Aobaku, Sendai, Miyagi, Japan
e-mail: y-ueno@med.id.yamagata-u.ac.jp;
yeuno@med.tohoku.ac.jp

Y. Tanaka
Virology and Liver Unit, Nagoya City University Medical
School, Nagoya, Japan

K. Kobayashi
Tohoku University Graduate School of Medicine,
2-1 Seiryo, Aobaku, Sendai, Miyagi, Japan

M. Miura
Department of Gastroenterology, South Miyagi Medical Center,
Oogawara, Miyagi, Japan

T. Yamamoto
Department of Gastroenterology, Tohoku Kosei-Nenkin
Hospital, Sendai, Miyagi, Japan

T. Kobayashi
Department of Hepatology, Tohoku Rosai Hospital,
Sendai, Miyagi, Japan

T. Igarashi
Department of Gastroenterology, Osaki Citizen Hospital,
Osaki, Japan

Introduction

Hepatitis B virus (HBV) and Hepatitis C virus (HCV) are noncytopathic viruses that cause chronic hepatitis and hepatocellular carcinoma (HCC) [1, 2]. HBV now affects more than 400 million people worldwide, and persistent infection develops in ~5 % of adults and 95 % of neonates who become infected with HBV [3]. HCV infects about 170 million people worldwide and is a major cause of chronic hepatitis, cirrhosis, and HCC [4]. Some groups have mentioned that dual infection with HBV/HCV is not uncommon in Asian patients [5, 6]. The prevalence of patients with dual HBV/HCV infection is approximately 10–15 %, although it likely differs among countries [7–9]. Co-infection with HBV/HCV has been associated with severe liver disease and frequent progression to cirrhosis [10]. Moreover, a significantly higher incidence of HCC and liver-related mortality was noted in patients with HBV/HCV co-infection [11, 12]. However, some groups reported, based on a meta-analysis, that dual infection with HBV/HCV did not increase the risk of HCC [13, 14]. These contradictory reports could be explained by the rarity of dual infection with HBV/HCV in patients without clinically evident liver disease. It might be difficult to estimate the hepatocarcinogenic risk of dual infection compared with that of either infection alone in such clinical settings [15].

An inverse relationship in the replicative levels of the two viruses has been noted, suggesting direct or indirect effects in vivo [16]. More recently, some groups have reported, using an in vitro infection system, that there is little direct interaction of HBV/HCV in coinfected hepatocytes [17, 18]. Therefore, the viral interference observed in coinfected patients is probably due to indirect mechanisms mediated by the innate and/or adaptive host immune responses.

The cellular immune response to HBV and HCV plays an important role in the pathogenesis of chronic hepatitis, cirrhosis, and HCC [19–21]. Hyporesponsiveness of HBV- or HCV-specific T-helper 1 cells and excessive regulatory function of $CD4^+CD25^+FoxP3^+$ regulatory T cells (Tregs) in peripheral blood have been shown in patients with chronic hepatitis B and C [22–34]. Recently, we reported that HBV replication stress could enhance the suppressive activity of Tregs via TLR2 [35]. However, little is known about the immunopathogenesis of HBV/HCV dual infection.

Dual infection can be classified into several groups (e.g., group A: HBV active and HCV active; group B: HBV inactive and HCV active; and group C: HBV active and HCV inactive) [36]. HCV is reported to be the dominant virus in HBV/HCV dual infection, but the dominance of either virus might be due to the genotypes of each virus and/or ethnic differences that could affect the proliferative activity of the viruses [36]. In this study, we investigated immunopathogenesis in a group A patient and in group B patients during therapy with pegylated interferon-α2b (Peg-IFN-α2b) plus ribavirin.

Patients, materials, and methods

Patients

One patient with high HBV-DNA and high HCV-RNA titers (HBV-high/HCV-high; patient A) and 5 patients with low HBV-DNA and high HCV-RNA titers (HBV-low/HCV-high) were enrolled (one of these patients, whose results were analyzed in detail, was termed patient B; see findings below in the "Results"). Twenty patients mono-infected with HBV and 10 patients monoinfected with HCV were enrolled as control subjects. None of the patients had liver disease due to other causes, such as alcohol, drugs, congestive heart failure, or autoimmune diseases. Permission for the study was obtained from the Ethics Committee at Tohoku University Graduate School of Medicine (permission no. 2006-194). Written informed consent was obtained from all the participants enrolled in this study. Participants were monitored for two years. At each assessment, patients were evaluated by biochemical laboratory tests, immunological analysis, and virological tests. Liver histology was analyzed at the start of Peg-IFN/RBV therapy by using laparoscopic liver biopsy samples and by employment of the METAVIR score.

Detection of interleukin (IL)-28B polymorphism

Genomic DNA was isolated from peripheral blood mononuclear cells (PBMCs) using an automated DNA isolation kit. Then polymorphism of IL-28B (rs8099917) was analyzed using real-time polymerase chain reaction (PCR) (TaqMan SNP Genotyping Assay, Applied Biosystems, CA, USA). Detection of the IL-28B polymorphism was approved by the Ethics Committee at Tohoku University Graduate School of Medicine (permission no. 2010-323).

Isolation of peripheral blood mononuclear cells (PBMCs) and flow cytometry

Peripheral blood mononuclear cells (PBMCs) were isolated from fresh heparinized blood by means of Ficoll-Hypaque density gradient centrifugation (Amersham Bioscience, Uppsala, Sweden). PBMCs were stained with CD3, CD4, CD8, CD19, CD25, CD40, CD56, CD86, HLA-DR, NKG2D, and isotype control antibodies (Becton Dickinson, NJ, USA) for 15 min on ice to analyze the frequency

of CD3$^+$CD4$^+$HLA-DR$^+$ cells, CD3$^+$CD8$^+$HLA-DR$^+$cells, CD4$^+$CD25$^+$ Tregs, CD3$^-$CD16$^-$CD56^{high}natural killer (NK) cells, and CD3$^-$CD16$^+$CD56^{dim} NK cells. The frequencies of the immune subsets were analyzed by flow cytometry using FACS Canto-II (Becton Dickinson, NJ, USA).

ELISPOT assay

The detection of IFN-γ and IL-10 was performed using an ELISPOT Set (BD Biosciences, San Jose, CA, USA) according to the manufacturer's instructions. Cultures of PBMCs were established in triplicate on round-bottomed 96-well plates for all time points investigated, at a concentration of 3 × 10^5 cells per well in 100 μl RPMI 1640 containing 10 % fetal bovine serum (FBS). Positive spots were detected using an automated counting machine.

Detection of HBV-DNA and determination of HBV genotype

DNA was extracted from 100 μl of serum using SMITEST EX-R&D (Medical & Biological Laboratories, Nagoya, Japan) and dissolved in 20 μl of nuclease-free distilled water. The DNA preparation thus obtained (10 μl) was subjected to nested PCR with primers targeting the S gene of the HBV-DNA, as described previously [37]. Briefly, first-round PCR was carried out for 35 cycles (98 °C for 10 s, 55 °C for 15 s, and 72 °C for 1 min, with an additional 7 min in the last cycle) in the presence of Prime-STAR HS DNA Polymerase (TaKaRa Bio, Shiga, Japan) and primers HB095 (sense, 5′-GAG TCT AGA CTC GTG GTG GAC-3′) and HB184 (antisense, 5′-CGA ACC ACT GAA CAA ATG GCA CCG-3′), for 25 cycles. This was followed by a second-round PCR consisting of 25 cycles using the same conditions as in the first round, with primers HB097 (sense, 5′-GAC TCG TGG TGG ACT TCT CTC-3′) and S2-2 (antisense, 5′-GGC ACT AGT AAA CTG AGC CA-3′). The HBV genotype was determined by phylogenetic analysis of the S gene sequence (437 nt) of the HBV isolates.

Detection of HCV RNA

RNAs were extracted from 250 μl of serum using TRIzol LS (Invitrogen, Tokyo, Japan). They were divided into two aliquots and each was assayed by reverse transcription (RT)-PCR with nested primers derived from the core region and NS5A interferon sensitivity determining region (ISDR) of the HCV genome. Nested PCR of the core region of the HCV genome was carried out with primers C008 (sense, 5′-AAC CTC AAA GAA AAA CCA AAC G-3′) and C011 (antisense, 5′-CAT GGG GTA CAT YCC GCT YG-3′) in

the first round and C009 (sense, 5′-CCA CAG GAC GTY AAG TTC CC-3′) and C010 (antisense, 5′-AGG GTA TCG ATG ACC TTA CC-3′) in the second round. Nested primers that were derived from NS5A-ISDR of the HCV genomes were designed to amplify a 188-bp product with C004 (sense, 5′-ATG CCC ATG CCA GGT TCC AG-3′) and C005 (antisense, 5′-AGC TCC GCC AAG GCA GAA GA-3′) in the first round, and C006 (sense, 5′-ACC GG A TGT GGC AGT GCT CA-3′) and C007 (antisense, 5′-GTA ATC CGG GCG TGC CCA TA-3′) in the second round.

Analysis of nucleotide and amino acid sequences

The PCR products were sequenced directly on both strands using a BigDye Terminator version 3.1 Cycle Sequencing Kit on an ABI PRISM 3100 Genetic Analyzer (Applied Biosystems, Foster City, CA, USA). Sequence analysis was performed using Genetyx-Mac ver. 12.2.6 (Genetyx, Tokyo, Japan) and ODEN (version 1.1.1) from the DNA Data Bank of Japan (National Institute of Genetics, Mishima, Japan) [38]. Sequence alignments were generated using CLUSTAL W (Version 1.8) [39]. The phylogenetic tree was constructed by the neighbor-joining method [40]. The reliability of the phylogenetic results was assessed using 1000 bootstrap replicants [41]. The final tree was obtained with the Njplot program (version 2.2) [42].

Plasmid construction

HBV expression plasmids were constructed by previously published methods. Serum samples were obtained from two patients infected with HBV genotype Bj and two patients infected with HBV genotype C. HBV-DNA was extracted from 100 μl serum using a QIAamp DNA blood kit (QIAGEN, Hilden, Germany). Four primer sets were designed to amplify two fragments covering the entire HBV genome. Amplified fragments were inserted into a pGEM-T Easy Vector (Promega, Madison, WI, USA) and cloned in DH5a competent cells (TOYOBO, Osaka, Japan). Briefly, at least 5 clones of each fragment were sequenced and the consensus sequence was identified and used as a template for 1.24-fold the HBV genome of different genotypes (B1 indicates the genotype Bj35 clone; B2 indicates the genotype Bj56 clone; C1 indicates the genotype C-AT clone; and C2 indicates the genotype C-22 clone). The HCV-JFH-1 strain was provided by Dr. T. Wakita (National Institute of Infectious Diseases, Japan).

HCV and HBV expression in Huh 7 cells

Cell-culture-derived infectious HCV was generated as described previously [43]. The HCV was quantified as

follows: RNA was extracted from the Huh-7 culture super-natant using a QIAamp Viral RNA Kit (Qiagen, Valencia, CA, USA). The HCV RNA was quantified by real-time RT-PCR, using TaqMan EZ RT-PCR Core Reagents (Applied Biosystems) according to the manufacturer's protocol, using the published primers and probe [44]. The filtered (0.45 μm) culture supernatant of HCV-infected Huh-7 cells containing 2×10^8 HCV RNA copies/ml [equivalent to 9.7×10^4 focus-forming units (ffu)/ml] was used for the experiments. To analyze HCV-RNA in the supernatant, Huh-7 cells (2×10^5 cells in a 6-well plate) were infected with JFH-1 (multiplicity of infection [MOI] = 0.01) and after 4 h the cells were washed twice with phosphate-buffered saline (PBS). The supernatants were then collected and the cells were reseeded at 2×10^5 cells per 6-well plate. Then the HBV expression and mock plasmid were transfected by FuGENE6 (Roche Applied Science, IN, USA). The super-natant of the culture medium was collected 72 h after transfection. Quantification of HBV-DNA and HCV-RNA was carried out using real-time PCR.

IFN-α was added 24 h after the transfection of the HBV plasmids, and the supernatant of the culture medium was then collected 48 h after the addition of the IFN-α.

Results

Clinical characteristics of patients A and B

Patient A (high HBV-DNA titer and high HCV-RNA titer)

Patient A was a 44 year-old man with a high aspartate aminotransferase/alanine aminotransferase (AST/ALT) level. The prothrombin time-international normalized ratio (PT-INR) was in the normal range. Patient A had high HBV-DNA titers and high HCV-RNA titers (Table 1). His liver histology was classified as A2/F3 (Fig. 1). The lapa-roscopic analysis indicated moderate inflammation and intermediate fibrosis. The liver surfaces of the right lobe and left lobe were almost the same phenotype. Polymor-phism of IL-28B (rs8099917) was T/G (hetero allele).

Patient B (low HBV-DNA titer and high HCV-RNA titer)

Patient B was a 63 year-old man with a low AST/ALT level. PT-INR was in the normal range. Patient B had low HBV-DNA titers and high HCV-RNA titers. The liver histology was classified as A2/F1 (Fig. 1). The liver sur-face showed moderate inflammation and was smooth. The polymorphism of IL-28B (rs8099917) was T/T (major homo allele).

Biopsy samples from patients with dual HBV and HCV infection were collected at the main liver centers in Miyagi

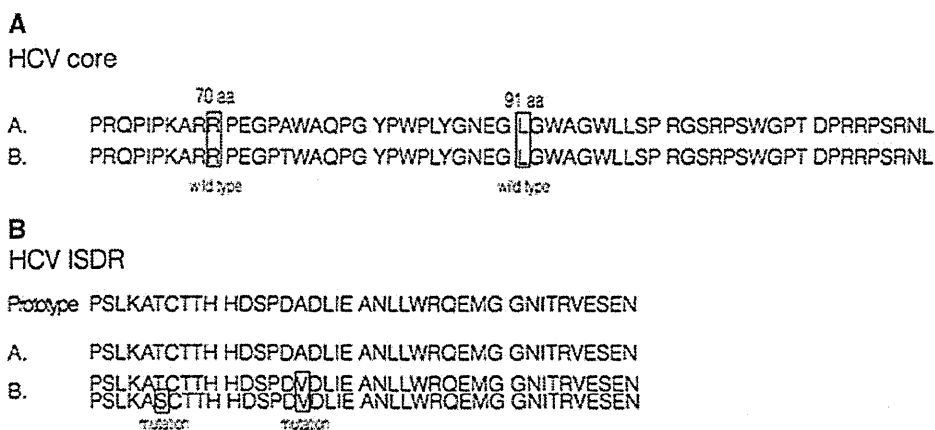**Table 1** Background of HBV/HCV dual-infected patients

	Patient A HCV high titer/ HBV high titer	Patient B HCV high titer/ HBV low titer	Normal range
Gender	Male	Male	
Age (years)	44	63	
HCV-RNA	6.5	5.5	log copies/ml
HCV genotype	1b	1b	
HBV-DNA	5.5	3.5	log copies/ml
HBV genotype	C	Bj	
HBe-Ag	129.5	0.5	0–0.9 index
HBe-Ab	0.1	99.3	0–49 %
Total bilirubin	0.7	1.2	0.2–1.2 mg/dl
Direct bilirubin	0.1	0.1	0–0.3 mg/dl
γ-GTP	208	31	8–57 IU/l
AST	138	33	12–30 IU/l
ALT	256	38	8–35 IU/l
Hb-A1c	5.3	5.4	4.3–5.8 %
Glu	103	83	68–106 mg/dl
BMI	25.34	18.75	
T-cho	160	195	128–220 mg/dl
LDL-cho	69	93	70–139 mg/dl
HDL-cho	37	67	36–89 md/dl
WBC	7800	5100	3200–9600/μl
RBC	491	446	$428–566 \times 10^4$/μl
Hb	17.1	14.1	13.6–17.4 g/dl
PLT	169000	176000	155000–347000/μl
PT-INR	0.87	0.96	0–1.15 INR
Liver histology	A2/F3	A2/F1	METAVIR score
IL-28B SNP (rs8099917)	T/G	T/T	

HCV hepatitis C virus, *HBV* hepatitis B virus, e-*Ag* envelope antigen, e-*Ab* envelope antibody, *γ-GTP* γ-guanosine triphosphate, *AST* aspartate aminotransferase, *ALT* alanine aminotransferase, *Hb* hemoglobin, *Glu* glucose, *BMI* body mass index, *T-cho* total cho-lesterol, *LDL* low-density lipoprotein, *HDL* high-density lipoprotein, *PLT* platelets, *PT-INR* prothromin time-international normalized ratio, *IL* interleukin, *SNP* single-nucleotide polymorphism

prefecture. Fifteen HBV/HCV dual-infected patients were found in this study (Supplementary Table 1). Many of these patients had HCV-dominant infection and undetect-able levels of HBV replication (10/15 patients). Most of the patients were HB envelope antigen (eAg)-negative and HBe antibody (Ab)-positive (14/14 patients). All HBV/HCV dual-infected patients who had received Peg-IFN-based
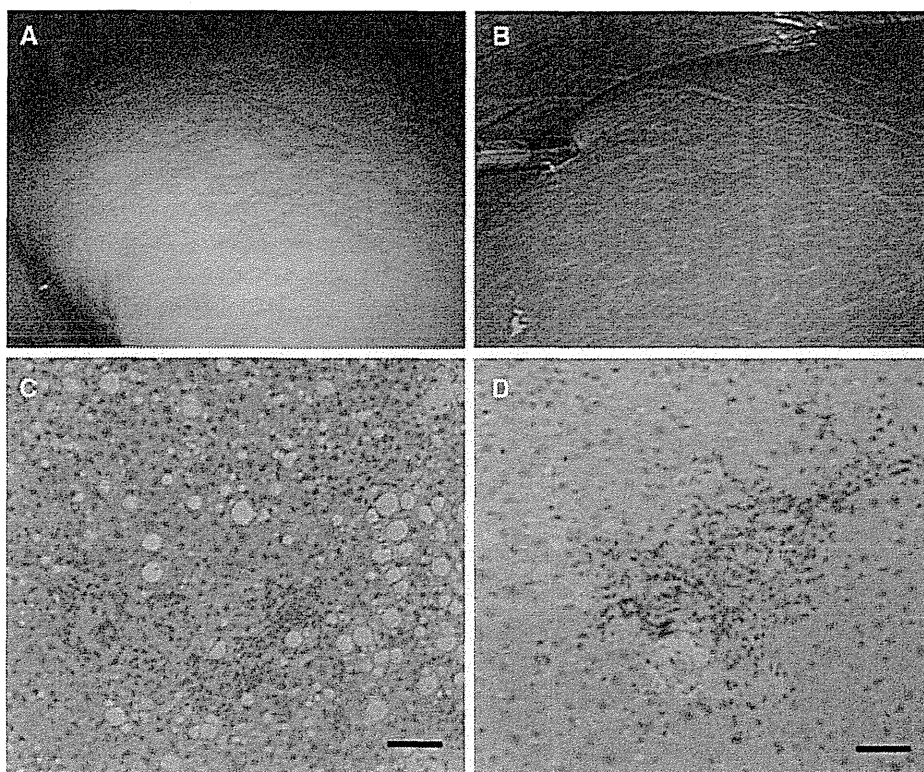
Fig. 1 Laparoscopic liver biopsy. The laparoscopic images of the liver surfaces of patient A (**a**) and patient B (**b**) are shown. Histopathology of patient A (**c**) and patient B (**d**) is also shown. *Bars* = 50 μm

A
HCV core


```
                70 aa                        91 aa
   A.     PRQPIPKAR PEGPAWAQPG YPWPLYGNEG  GWAGWLLSP RGSRPSWGPT DPRRPSRNL
   B.     PRQPIPKAR PEGPTWAQPG YPWPLYGNEG  GWAGWLLSP RGSRPSWGPT DPRRPSRNL
              wild type                        wild type
```

B
HCV ISDR

```
Prototype  PSLKATCTTH HDSPDADLIE ANLLWRQEMG GNITRVESEN

   A.      PSLKATCTTH HDSPDADLIE ANLLWRQEMG GNITRVESEN

   B.      PSLKATCTTH HDSPDVDLIE ANLLWRQEMG GNITRVESEN
           PSLKASCTTH HDSPDVDLIE ANLLWRQEMG GNITRVESEN
              mutation      mutation
```

Fig. 2 Virological analysis of hepatitis B virus (HBV) and hepatitis C virus (HCV) in HBV/HCV dual infection. The amino acid sequences of the HCV-core region including core-70 and core-91, which were previously reported as determinants of the sensitivity to pegylated interferon/ribavirin (Peg-IFN/RBV) therapy, in patient A and patient B are shown (**a**). The amino acid sequences of the interferon sensitivity determining region (*ISDR*), which were previously reported as determinants of the sensitivity to IFN, in patients A and B are shown (**b**)

treatment achieved a sustained viral response (SVR) (5/5 patients). These data indicated that HCV-dominant dual-infected patients had good responses to treatment for HCV infection.

Virological analysis of HBV/HCV in patients A and B

The HCV genotype in both patient A and patient B was 1b. The sequences of amino acids in the ISDR region and HCV

core-70 and core-91 amino acids were analyzed by direct sequencing. Both patients had wild-type core-70 and core-91 amino acids (Fig. 2a). None of the mutations of the ISDR region was detected in patient A, but two of the mutations of the ISDR region were detected in patient B (Fig. 2b). The genotypes of HBV in patients A and B were analyzed by direct sequencing and phylogenetic tree analysis. The genotype of HBV in patient A was genotype C, which has been reported as difficult-to-treat HBV. The genotype of HBV in patient B was genotype Bj, which has been reported as easy-to-treat HBV in comparison to genotype C [45–47].

Sequential analysis of biochemical and virological data during Peg-IFN/RBV therapy

Patient A

In patient A, HCV-RNA gradually declined during Peg-IFN/RBV therapy. On the other hand, the HBV-DNA gradually increased during Peg-IFN/RBV therapy (Fig. 3a). The amount of HBeAg started to increase 9 months after the start of Peg-IFN/RBV therapy. HCV-RNA started to increase 12 months after the start of Peg-IFN/RBV therapy, although Peg-IFN/RBV was still being administered up to 18 months after the start of Peg-IFN/RBV therapy (Fig. 3a).

Patient B

In patient B, HCV-RNA and HBV-DNA rapidly declined after the start of Peg-IFN/RBV therapy (Fig. 3b). HCV-RNA could not be detected in peripheral blood 2 months after the start of Peg-IFN/RBV therapy. Peg-IFN/RBV was administered up to 12 months after the start of the Peg-IFN/RBV therapy. The amounts of HBeAb and HBeAg did not change during the Peg-IFN/RBV therapy (Fig. 3b).

Sequential immunological analysis during Peg-IFN/RBV therapy

We analyzed various subsets of immune cells that could affect the immunopathogenesis of HBV/HCV dual infection. NK cells ($CD3^-CD16^-CD56^{high}$ and $CD3^-CD16^+$ $CD56^{dim}$) and NK-T cells ($CD3^+CD56^+CD16^+$, $CD3^+$ $CD56^+CD16^-$ and $CD3^+CD56^-CD16^+$) were analyzed (Supplementary Fig. 1A). The $CD3^-$ gated lymphocytes were separated into 4 groups (a, b, c, and d). For these subsets, (a) indicated the presence of $CD3^-CD16^-CD56^{high}$ NK cells that could produce various cytokines vigorously and had low cytotoxic activity. Subset (b) showed $CD3^-CD16^+CD56^{dim}$ NK cells that had weak cytokine production ability and high cytotoxic activity.
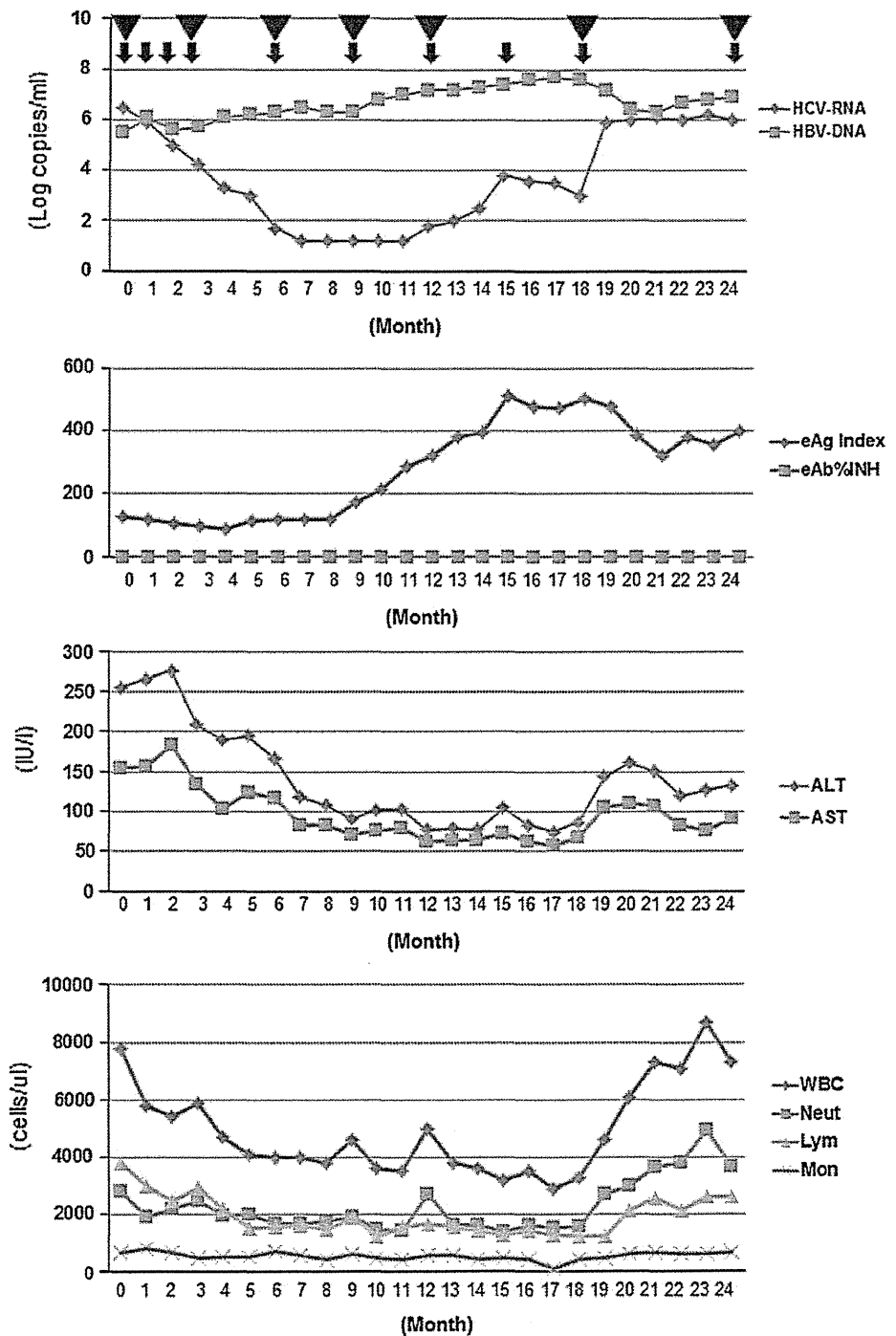
The $CD3^+$ gated lymphocytes were separated into 3 groups (a, b, and c). The activated $CD3^+$, $CD3^+CD4^+$, and $CD3^+CD8^+$ T cells were analyzed (Supplementary Fig. 1B). HLA-DR$^+$ activated $CD3^+$, $CD3^+CD4^+$, and $CD3^+CD8^+$ T cells could be clearly distinguished by FACS analysis. Additionally, representative dot plots of Tregs and B cells were created (shown in Supplementary Fig. 1C). The frequencies of $CD3^-CD16^+CD56^{dim}$ NK cells, $CD3^+CD16^-CD56^+$ NK-T cells, activated $CD3^+CD4^+$ T cells, and activated $CD3^+CD8^+$ T cells fluctuated similarly during Peg-IFN/RBV therapy in patient A (Supplementary Fig. 1D). Activated T cells were increased at one month of Peg-IFN/RBV therapy, and the above subsets of lymphocytes gradually decreased up to 3 months of Peg-IFN/RBV therapy. After that, these cells gradually increased again up to 9 months of Peg-IFN/RBV therapy. In patient A, after 9 months of Peg-IFN/RBV therapy, these cells had decreased again (Supplementary Fig. 1D). The frequency of Tregs and activated B cells (data not shown) did not change during Peg-IFN/RBV therapy in patient A (Supplementary Fig. 1D). On the other hand, in patient B, the frequencies of $CD3^-CD16^+$ $CD56^{dim}$ NK cells, $CD3^+CD16^-CD56^+$ NK-T cells, activated $CD3^+CD4^+$ T cells, and activated $CD3^+CD8^+$ T cells were increased and sustained during Peg-IFN/RBV therapy (Supplementary Fig. 1E). Five HCV monoinfected patients were analyzed by the same protocol (Supplementary Fig 1F). The mean frequency of various kinds of immune subsets was analyzed (Supplementary Fig 1F). The tendency of immunological reactions during Peg-IFN/RBV therapy in these five patients was similar to that in patient B.

Analysis of HBV- and HCV-specific immune responses

The analysis of HBV- and HCV-specific-immune responses was carried out by ELISPOT assay. Representative spots of IFN-γ are shown in Fig. 4a. In patient A, HCV- and HBV-specific IFN-γ secretion activities were remarkably low in comparison to the IL-10 secretion activity. Moreover, in patient A, the induction of IFN-γ-secreting cells could not be detected after Peg-IFN/RBV therapy, especially in regard to HBV-core specific IFN-γ secretion in PBMCs (Fig. 4b). On the other hand, in patient B, the HBV-core specific IFN-γ-secreting cells were high in comparison to those in patient A (Fig. 4c). Moreover, the induction of IFN-γ-secreting cells could be detected during Peg-IFN/RBV therapy in patient B (Fig. 4c). The mean numbers of IFN-γ- and IL-10-secreting spots in HBV-dominant dual-infected patients, patients with monoinfection with HBV genotype Bj (HBeAb$^+$), Bj (HBeAg$^+$), C (HBeAb$^+$), C (HBeAg$^+$), or HCV genotype 1b are shown in Fig. 4d. In patient A, HB core antigen (HBcAg)-specific IFN-γ secretion was weaker than that in

Fig. 3 Sequential biochemical data analysis during Peg-IFN/RBV therapy. The titers of HBV-DNA and HCV-RNA; the amounts of envelope antigen (*eAg*) and envelope antibody (*eAb*), and alanine aminotransferase (*ALT*) and aspartate aminotransferase (*AST*); and the numbers of WBCs, neutrophils (*Neut*), lymphocytes (*Lym*), and monocytes (*Mon*) in patients A (a) and B (b) are shown in these graphs. *Arrows* indicate the sampling points of FACS analysis. *Triangles* indicate the sampling points of the ELISPOT assay. *INH* inhibition

HBV-genotype C-monoinfected patients who were HBeAg-positive. However, HBcAg-specific IL-10 secretion in patient A was stronger than that in HBV-genotype C monoinfected patients who were HBeAg-positive. These data indicated that the presence of HCV might also suppress the HBV-specific immune response in regard to certain host factors (e.g., in the presence of IL-28B polymorphism, and depending on the body mass index [BMI] and γ-guanosine triphosphate [γ-GTP] level), because the presence of HCV did not suppress the HBV-specific immune response either in patient B or in the patients with dual HCV-dominant infection. Otherwise, we could deny the possibility indicating that

Fig. 3 continued

**B HCV High/HBV Low [Sequential Biochemical Data During PEG-IFNα+RBV Therapy]**
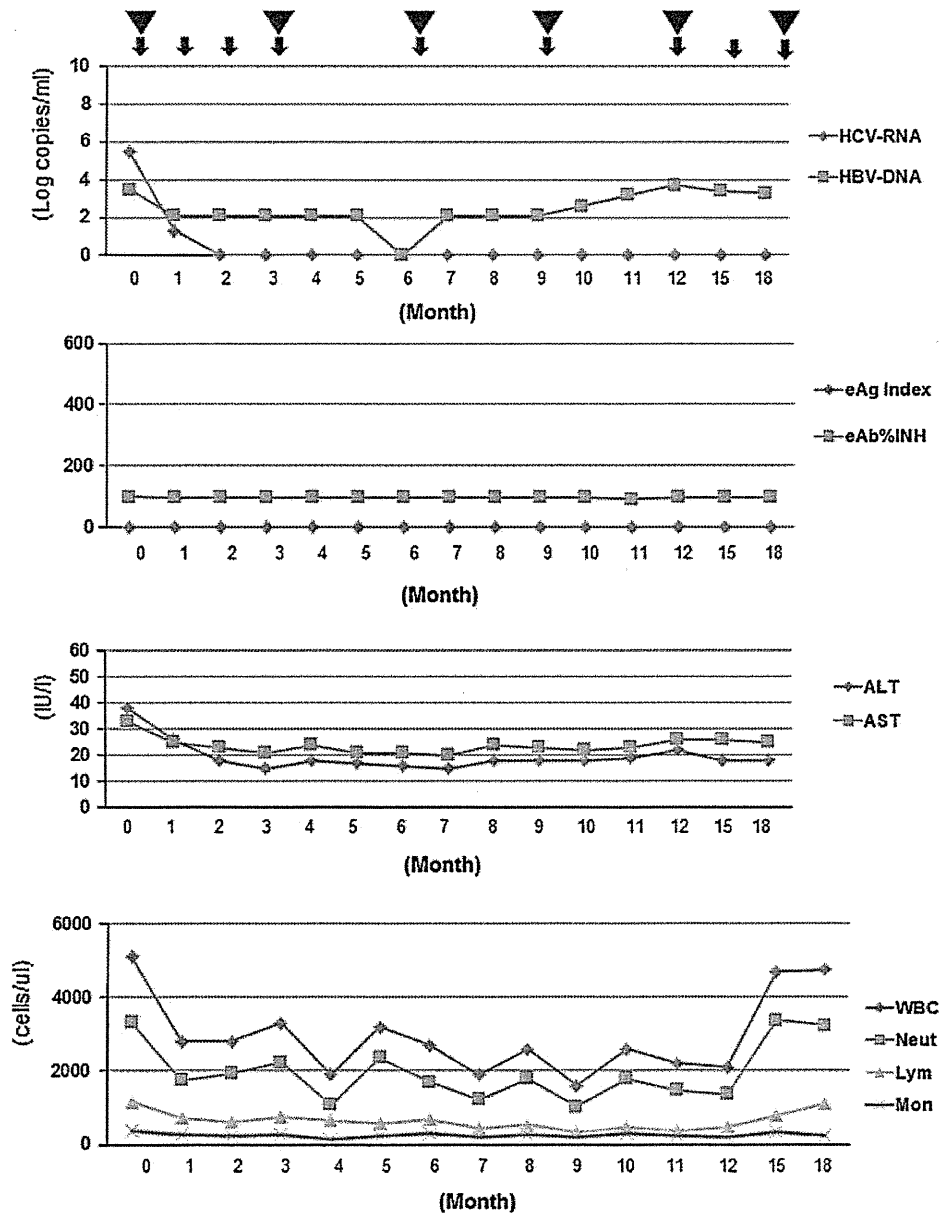
the certain background of host factors could allow the existence of dual virus actively. These data indicated that HBV-specific IL-10-secreting cells and/or certain kinds of host factors had an important role in HBV- and HCV-specific immune suppression in patient A, but not in patient B.

In vitro analysis of HBV/HCV dual infection

We carried out in vitro analysis of HBV/HCV infection using Huh-7 cells that were susceptible to the HCV-JFH-1 strain

and HBV expression plasmids. The amount of the JFH-1 strain did not change with the various kinds of HBV expression plasmids (Fig. 5a). Moreover, the amounts of the various HBV strains did not change in the presence of JFH-1 infection. These data indicated that no direct effect of HBV and HCV could be detected in Huh 7 cells. We carried out experiments to analyze the effect of IFN-α treatment on HCV Huh-7 cells with various kinds of HBV expression (Fig. 5b). In our systems, it appeared that HBV expression could not significantly affect the suppressive effect of IFN-α.
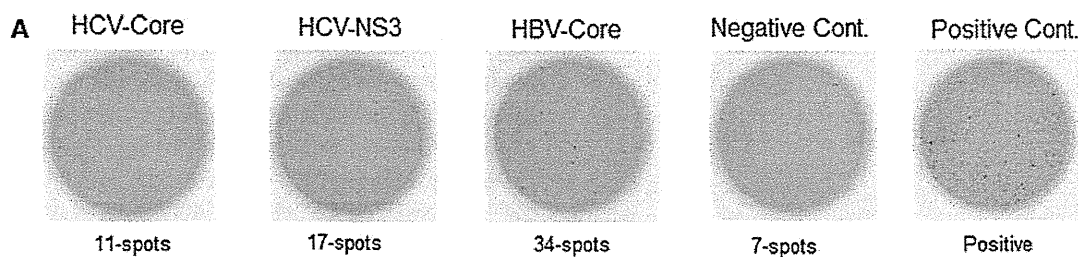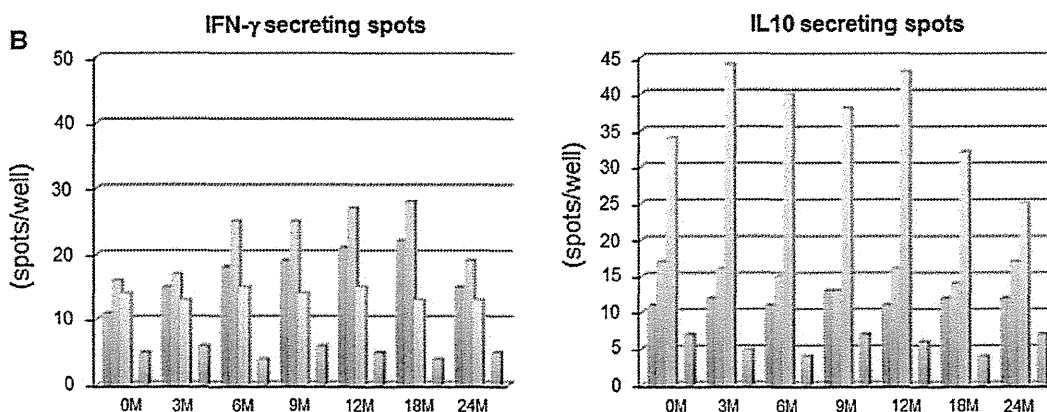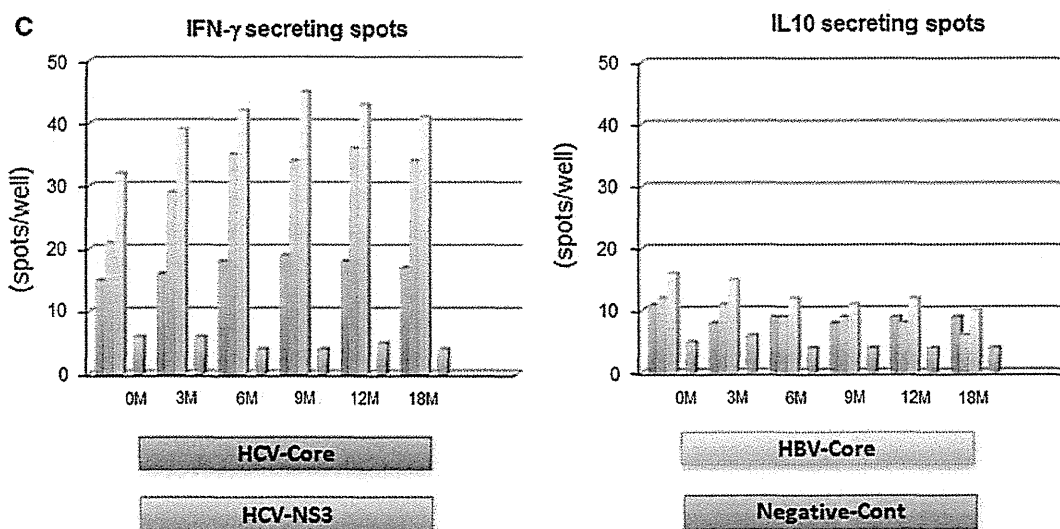
Fig. 4 The sequential analysis of HBV/HCV-specific immune reactions during Peg-IFN/RBV therapy. Representative spots of the ELISPOT assay are shown (**a**). The sequential data of IFN-γ- and interleukin-10 (*IL-10*)- secreting spots in patient A are shown (**b**). The sequential data of IFN-γ- and IL-10-secreting spots in patient B are shown (**c**). Comparison of IFN-γ- and IL-10- secreting spots in patient A before starting therapy, patient B before starting therapy, dual HCV-dominant patients, HCV-monoinfected patients, HBV-Bj (HBeAb$^+$) monoinfected patients, HBV-Bj (HBeAg$^+$) monoinfected patients, HBV-C (HBeAb$^+$) monoinfected patients, and HBV-C (HBeAg$^+$) monoinfected patients (**d**). In these *bar graphs*, the *blue bars* indicate HCV-core specific reaction. The *red bars* indicate HCV-NS3 specific reaction. The *green bars* indicate HBV-core specific reaction. The *aqua blue bars* indicate the negative control (*Cont.*). *Error bars* indicate standard deviations (color figure online)